Jurnal Teknologi

Full Paper

COMPARISON OF FLOW FIELD BETWEEN STEADY AND UNSTEADY FLOW OF AN AUTOMOTIVE MIXED FLOW TURBOCHARGER TURBINE

M.H. Padzillah[a*], S. Rajoo[a], R.F. Martinez-Botas[b]

[a]UTM Centre for Low Carbon Transport in cooperation with Imperial College London, Faculty of Mechanical Engineering Universiti Teknologi Malaysia, 81310 UTM Johor Bahru, Malaysia
[b]Department of Mechanical Engineering, Imperial College London, London SW7 2AZ, United Kingdom

Article history
Received
1 January 2016
Received in revised form
18 May 2016
Accepted
15 June 2016

*Corresponding author
mhasbullah@utm.my

Graphical abstract

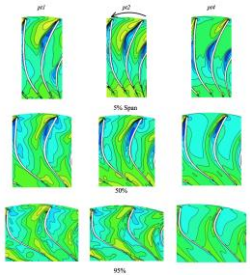

Abstract

Global decarbonizing efforts in transportation industry have forced the automotive manufacturers to opt for highly downsized high power-to-weight ratio engines. Since its invention, turbocharger remains as integral element in order to achieve this target. However, although it has been proven that a turbocharger turbine works in highly pulsatile environment, it is still designed under steady state assumption. This is due to the lack of understanding on the nature of pulsating flow field within the turbocharger turbine stage. This paper presents an effort to visualize the pulsating flow feature using experimentally validated Computational Fluid Dynamics (CFD) simulations. For this purpose, a lean-vaned mixed-flow turbine with rotational speed of 30000 rpm at 20 Hz flow frequency, which represent turbine operation for 3-cylinder 4-stroke engine operating at 800 rpm has been used. Results indicated that the introduction of pulsating flow has resulted in more irregular pattern of flow field as compared to steady flow operation. It has also been indicated that the flow behaves very differently between pressure increment and decrement instances. During the pressure decrement instance, flow blockage in terms of low pressure region occupies most of the turbine passage as the flow exit the turbine.

Keywords : Mixed-flow turbine, computational fluid dynamics, pulsating flow

Abstrak

Usaha mengurangkan pelepasan karbon secara global dalam industry pengangkutan telah menjadikan pengeluar kenderaan automotif memilih untuk menghasilkan enjin yang mempunyai nisbah kuasa-kepada-berat yang tinggi. Sejak penciptaannya, pengecas turbo masih kekal menjadi elemen penting untuk mencapai matlamat ini. Namun begitu, sungguhpun telah dibuktikan bahawa alat ini sentiasa beroperasi dalam keadaan aliran berdenyut, ianya masih lagi direka menggunakan andaian aliran mantap. Ini adalah kerana kurangnya kefahaman terhadap persekitaran aliran denyutan dalam pengecas turbo tersebut. Kertas kerja ini membentangkan satu usaha untuk memaparkan ciri-ciri aliran denyut menggunakan kaedah Pengiraan Dinamik Bendalir (CFD) yang telah disahkan secara uji kaji. Untuk tujuan ini, turbin aliran campuran dengan kelajuan putaran 30000 rpm pada frekuensi aliran 20 Hz, bagi mewakili operasi turbin pada enjin 3-silindir 4 lejang yang beroperasi pada 800 rpm telah digunakan. Keputusan menunjukkan bahawa pengenalan aliran berdenyut telah menyebabkan corak aliran yang lebih tidak teratur berbanding operasi aliran mantap. Keputusan juga telah menunjukkan bahawa corak aliran adalah sangat berbeza antara sewaktu tekanan sedang menaik dan menurun. Semasa tekanan sedang menurun, aliran didapati terganggudi mana kawasan tekanan rendah telahmeliputi sebahagian besar laluan turbin semasa aliran hamper dengan bahagian keluaran turbin.

Kata kunci: Turbin aliran campuran, dinamik bendalir berbantukan komputer,

1.0 INTRODUCTION

The complex nature of flow field interaction within the turbocharger turbine operating under pulsating flow condition has been one of the limiting factors towards the development of highly efficient turbine for internal combustion engine. Despite the need for expensive computing requirement to model such behaviour, there have been several attempts to visualise the flow field by means of CFD.Nevertheless, as experimental measurement of instantaneous parameters such as mass flow rate is rather difficult to conduct, many of these early numerical works were not validated.

Perhaps the earliest successful pulsating flow CFD simulation work was that of Lam et al.[1]. The main aim of this work was to demonstrate the capability of CFD to provide a sufficient description of the flow within the nozzles and the turbine passage. Lam et al. utilized the Multiple Rotating Frames (MRFs) method which is also known as the `frozen rotor' approach, which assumes no relative movement between stationary and rotating frames of reference during the simulations. One of the issues was the difficulty of getting the simulation to converge properly therefore only qualitative comparisons could be made. Furthermore, the complex geometry of the turbine itself presented a difficulty in defining the exact entry point of unsteady flow at the rotor inlet. Despite that, the work of Lam proved that it was possible to further understand the complexity of pulsating flow by means of full 3-D CFD.

Palfreyman and Martinez-Botas[2] improved the CFD work on pulsating flow by utilizing 'sliding-plane' interface between stationary and rotating domain. They indicated that the method leads to more accurate prediction and proved it by extensive validation procedure with the work of Karamanis[3]. Palfreyman and Martniez-Botas indicated that the flow field in the turbine passage under pulsating flow condition is highly disturbed. They also shown that the effect of blades passing the volute tongue effect the flow mostly in the inducer region. The poor flow guidance at the turbine inlet and exit has also been observed and attributed to the assumption of quasi-steady conditions during the design stage of the turbine.

Another work that extensively used CFD approach to simulate flow field behaviour is conducted by Hellstrom and Fuchs[4]. They varied the inlet condition of the turbine volute by introducing disturbances such as turbulence and swirls to see their effect on the turbine performance. Hellstrom and Fuchs indicated that turbulence and swirls effect the flow by introducing additional pressure loss and unfavourable radial velocity distribution respectively. These ultimately result in the reduction of power generation capability of the turbine. Despite successful simulation procedures with high number of node counts, the work of Hellstrom and Fuchs was not validated experimentally.

Recent work by Copeland et al. [5] utilized CFD approach in an attempt to characterize the level of 'unsteadiness' within the turbocharger turbine stage. This is done by defining a new parameter called 'lambda parameter' that represents the ratio of the time-averaged rate of change of the mass flow within the domain to the time-averaged of the through flow mass. This work indicated that the rotor stage is not wholly quasi-steady but is insignificant enough as compared to the volute stage. Building on the work of Copeland, Newton[6] indicated that the overall entropy generation in the pulsating case was 1.66% higher than the corresponding steady state condition, and could be attributed primarily to an increase in entropy generation in the nozzle-rotor interspace region.

The work presented in this paper aims to provide readers on the flow field behaviour within the turbocharger turbine stage under pulsating flow condition. Comparison of the flow field between steady and pulsating flow at similar level of pressure is also presented.

2.0 METHODOLOGY

2.1 Experimental Methodology

Figure 1 shows the schematics of the cold-flow turbocharger test facility used in this research

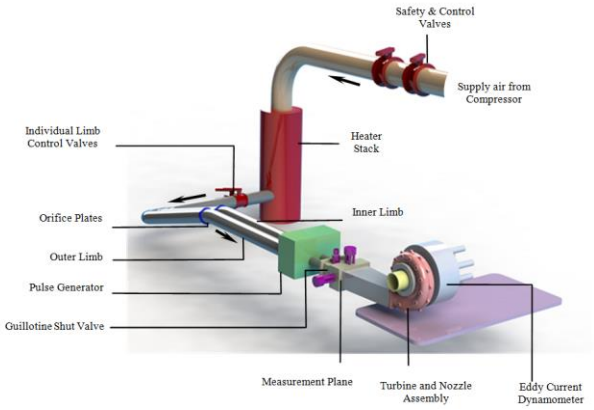

Figure 1 Imperial College 'cold flow' turbocharger test facility

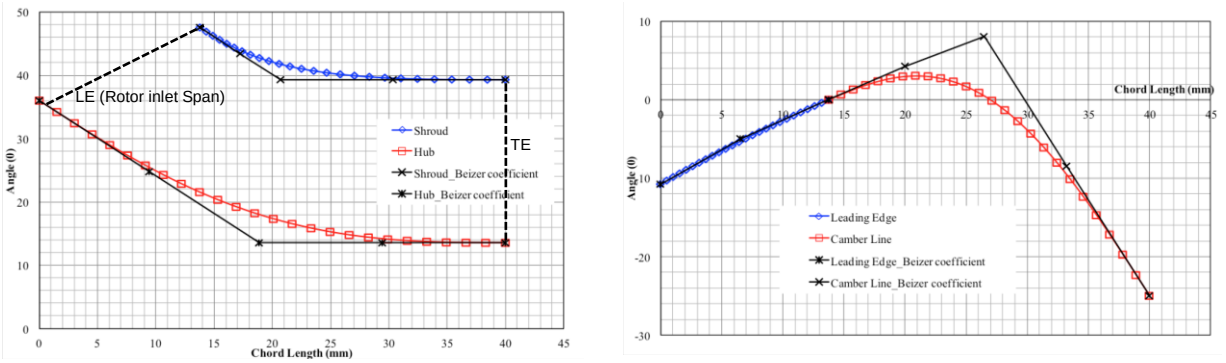

(a) (b)

Figure 2 Development of turbine geometry using Bezier Polynomial

located at Imperial College London. This facility, which is originally developed by Dale and Watson [7] is fully equipped to be used for both steady and pulsating flow testing. The compressed air for the test rig is supplied by three screw-type compressors with capacity up to 1 kg/s at maximum absolute pressure of 5 bars. Before the air flow is channelled into two 81.40mm limbs, it is pre-heated to 345 K to prevent condensation during air expansion in the turbine. The two limbs enable testing not only for single entry turbine but also for multiple entry turbine. The mass flow rate in both limbs is measured using both the electronic v-cone flowmeter as well as the orifice plates. Downstream the orifice plates is a specially cut-out pulse generator originally designed by Dale and Watsonin 1986. The pulse generator allows for replication of the actual pressure pulse inthe exhaust manifold. It is capable of generating pulses up to 80 Hz. For the steady flow testing, the pulse generator is defaulted to 'fully open' position to allow maximum steady-state flow area. Downstream the pulse generator is the 'measurement plane' that consist of a few measurement devices. This includes instantaneous pressure sensors, hotwire anemometer and thermocouples.

The turbine is attached to a 60kW eddy current dynamometer originally developed by Szymko[8]. The reaction force on the dynamometer assembly is measured by a 20kg load cell on the gimbal-mounted dynamometer housing. The heat that is released by the dynamometer stator is heavily cooled by a water cooling system. The temperature of the stator plate is constantly monitored and electronically linked to the mainframe for automatic shut-down in case of overheating. The dynamometer also places an optical sensor for the purpose of instantaneous speed measurement.

2.2 Numerical Methodology

The numerical works conducted in the current research utilized a commercial CFD software Ansys CFX 14.1. There are in total of 4 main components involved in building the solid model of the turbocharger turbine geometry. These components are known as a 40mm chord length mixed flow turbine, 15 stationary vanes, a modified Holset H3B volute[9] and also the inlet duct. The constructions of these individual components differ accordingly. The components that are directly related with rotordynamics such as the rotor and vanes are created in TurboGrid. This is done by specifying profile lines that contains Cartesian coordinates of hub, shroud and blade. 3 profile lines were specified in the construction of the nozzle blade. Meanwhile, due to its geometrical complexity, 8 profile lines are specified in the construction of the rotor. These lines were generated earlier using Bezier polynomial with the control points specified by Abidat [10] in 1991 to suit high loading turbine operation. Figure 2(a) shows the resultant polynomial lines that forms hub (blue line) and shroud (red line) of the rotor wheel. The dotted line in Figure 2(a) indicated the imaginary position of the leading and trailing edge of the rotor. It can be seen that the overall chord length is 40 mm. Figure 2(b) shows the curvature for leading edge and camber

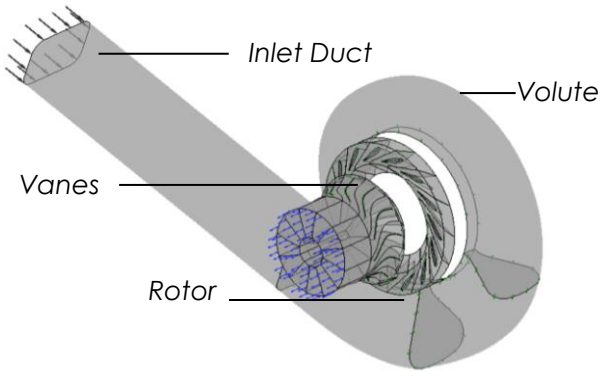

Figure 3 Assembly of domain in CFX-Pre

line of the blade. Meanwhile, the constructions of general components such as inlet duct and turbine volute were done using Solidworks. These solid models are then transferred into mesh generation software ICEM CFD. This software allows for specification of hexahedral mesh throughout the whole geometry.

After the meshing process of each of the components is completed, they we assembled to form a complete domain in Ansys CFX-Pre. This process is shown inFigure 3. For the specification of interface, the connections between stationary parts are defined as general connection. Meanwhile, the connecting surface between rotor (rotating) and stationary vanes is defined as the transient-rotor stator interface. This allows for relative movement between rotor and stator thus resulted in more accurate flow prediction.

The boundary conditions at inlet require the specification of either mass flow rate or total pressure. For current work, the time varying total pressure and temperature are set at this particular inlet location. The inlet parameters are area averaged at the inlet surface so that it only changes temporally. The values of these parameters were obtained at the measurement plane earlier during the experimental procedure. The direction of inlet flow is defined so that the only velocity component that exists is normal to the inlet plane. At the outlet boundary, static atmospheric pressure is specified. At the walls, no-slip boundary condition is set. This includes the wall of vanes and rotor blades. Due to the availability of experimental data at 30000rpm rotor rotation (equivalent to 50% design speed), it is decided that this speed are to be used to enable direct comparison with existing data.

3.0 RESULTS AND DISCUSSION

3.1 Validation Procedure

Before the analysis is conducted, the computed models are validated with experimental results. This procedure is done by computing the turbine performance parameters which are the turbine efficiency, velocity ratio, mass flow parameter (also known as swallowing capacity) and pressure ratio from CFD results and comparing them with actual experimental data.

The equations to obtain these parameters are shown in Equation 1 to 7

$$Pressure\ Ratio, PR = \frac{P_{01}}{P_5} \quad (1)$$

$$Mass\ Flow\ Parameter, MFP = \frac{\dot{m}\sqrt{T_{01}}}{P_{01}} \quad (2)$$

$$Total - to - static\ efficiency, \eta = \frac{W_{act}}{W_{isen}} \quad (3)$$

$$Actual\ Power, W_{act} = 2 \cdot \pi \cdot N \cdot \tau \quad (4)$$

$$Isentropic\ Power, W_{isen} = \dot{m} \cdot c_p \cdot T_{01}\left[1 - \left(\frac{P_5}{P_{01}}\right)^{\frac{\gamma-1}{\gamma}}\right] \quad (5)$$

$$Velocity\ Ratio, VR = \frac{U}{C_{is}} \quad (6)$$

$$Isentropic\ velocity, C_{is} = \sqrt{2 \cdot \frac{W_{isen}}{\dot{m}}} \quad (7)$$

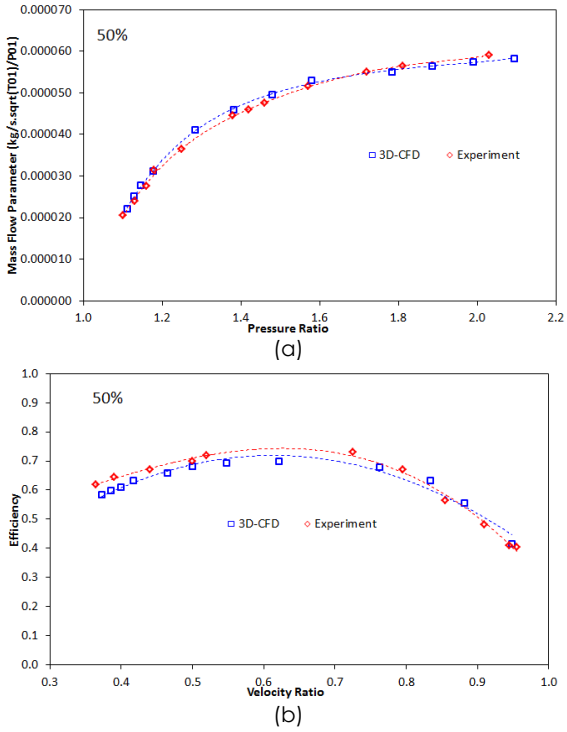

Figure 4 Comparison between CFD and Experimental data of (a) Mass Flow Parameter vs Pressure Ratio and (b) Efficiency vs Velocity Ratio

The plot of comparison between mass flow parameter against pressure ratio for CFD and experimental data is shown in Figure 4(a). Figure 4(a) indicated that the developed numerical model is able to capture both trend and magnitude of the turbocharger turbine mas flow parameter sufficiently well throughout the range of operation. The calculated Root Mean Square of the deviation is recorded to be 2%.

Meanwhile, the comparison process between CFD and experimental data for efficiency is relatively more challenging than that of mass flow parameter. This is due to its dependency of multiple parameters such as mass flow rate, total temperature, torque and also pressure. Any deviation on these parameters would enhance the differences of the calculated and measured efficiency values. The application of constants such as the specific heat value could also potentially effect accuracy of the prediction. The comparison between CFD and experimental data of

the efficiency plot is shown in Figure 4(b). In this plot, it can be observed that CFD recorded under prediction of the efficiency value at velocity ratio 0.85 and below. This deviation achieved its maximum value at 0.36 velocity ratio where the predicted efficiency is 5 points higher than experimentally measured value. The overall deviation indicated by Root Mean Square value is 2 efficiency points. In general, despite recorded deviations, the prediction points are well below the experimental uncertainty limits and as such is sufficiently accurate for the flow field analysis.

3.2 Flow Field Behaviour

In order to visualize the details of the flow field within the passage, the pressure and velocity contour are plotted for a few spanwise planes for all four conditions of interest. Three spanwise planes at 5%, 50% and 95% spanwise location are selected and the positions of these planes are visualized in Figure 5.Figure 6 shows the instances that the analysis is focused on. Pt1 and pt2 is the instances at similar level of pressure during pressure increment and decrement period respectively. Pt4 also has similar pressure level but the turbine is operating under steady state condition. Meanwhile, pt3 indicated maximum pressure at the particular operation frequency.

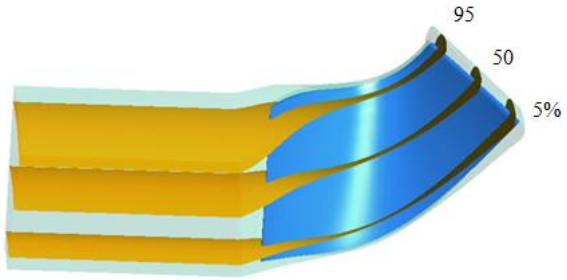

Figure 5 Orientation of blade-to-blade planes

Figure 7shows the pressure contour plot for pt1, pt2 and pt4 at different blade-to-blade planes. It is clear from Figure 7that the distribution of pressure field is significantly different from each other, albeit similar total pressure at the vanes inlet. The pressure field distribution for both pt1 and pt2 appear to be less uniform as compared to pt4 at all spanwise planes. It is also evidence from Figure 7that the low pressure (flow separation) region close to the suction surface within the passage is larger during the pressure decrement period (pt2) than the pressure increment (pt1) period during a pulse. The worst distribution of pressure field occur at pt1 and pt2 at 95% blade-to-blade plane due to the combined effect of tip leakage flow as well as the unsteadiness of the incoming flow. Even though there is a large low pressure region near the suction surface at 95% blade-to-blade plane for the steady condition (pt4), this region is limited only close to the suction surface until the flow reaches the rotor trailing edge. On the other hand, other conditions especially pt2 indicated that the low pressure region keeps growing and occupies most of the passage as the flow exit the turbine.

Figure 8 shows the velocity contour for pt1, pt2 and pt4 at different blade-to-blade plane. Since the selected inlet total pressure for the comparison of these three conditions are at higher-than-optimum pressure, one would expect that the velocity field distribution within the rotor passage is not uniformly distributed. This behaviour occurs due to positive incidence angle as well as its non-uniformity at the rotor inlet. Despite that, it is still obvious in Figure 8that the velocity distribution at pt1 and pt2 are more irregular than its distribution at pt4. As expected from the analysis of pressure contour in Figure 7, the velocity distribution of pt1 (increasing pressure) is rather different than pt2 (decreasing pressure). Another interesting phenomenon that can be seen in Figure 8is the comparison of the velocity contour behaviour at 5% spanwise location between steady(pt4) and unsteady(pt1 and pt2) conditions. At pt4, it can be seen that the low velocity region emerged at about 30% up to 60% streamwise location close to the suction surface whereas for the other two unsteady conditions (pt1 and pt2), the low velocity region emerged close to the leading edge of the rotor up to about 50% streamwise location, also close to the suction surface.

The second part of the flow field comparison involves the three unsteady conditions, which are pt1, pt2 and pt3. The pressure contours for these conditions are plotted in Figure 9. It can be seen that during pulsating flow conditions, the pressure distribution is distorted at all times especially close to the shroud wall (95% span) due to the reason explained before. At high pressure ratio (pt3), the region of low pressure at 5% spanwise location seems to be occupying half the passage pitch at 20% streamwise but also bounded only up to about 40% streamwise location close to the suction surface.

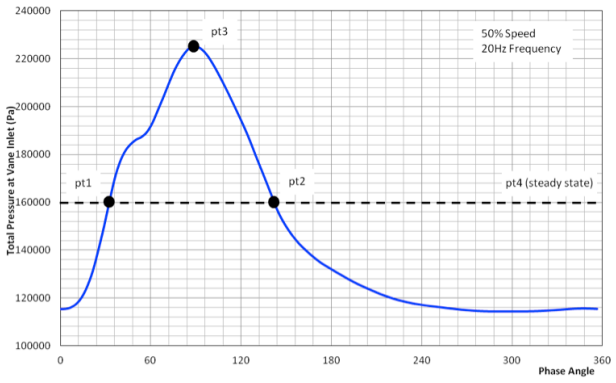

Figure 6 Steady and unsteady operating condition for flow field analysis

Another interesting observation is that the low pressure region that exists in pt3 which is mostly close to the suction surface is very close in terms of its magnitude to the low pressure region recorded in pt1 and pt2.

Figure 10 shows the velocity contour at different spanwise planes for pt1, pt2, and pt3. At 5% spanwise location, it can be seen that there is a low velocity region close to the suction surface and originated from the leading edge for all the conditions. This is one of the key differences in the velocity profile between pulsating and steady turbine operations where the low velocity occurs slightly downstream during steady operations as indicated in Figure 8.

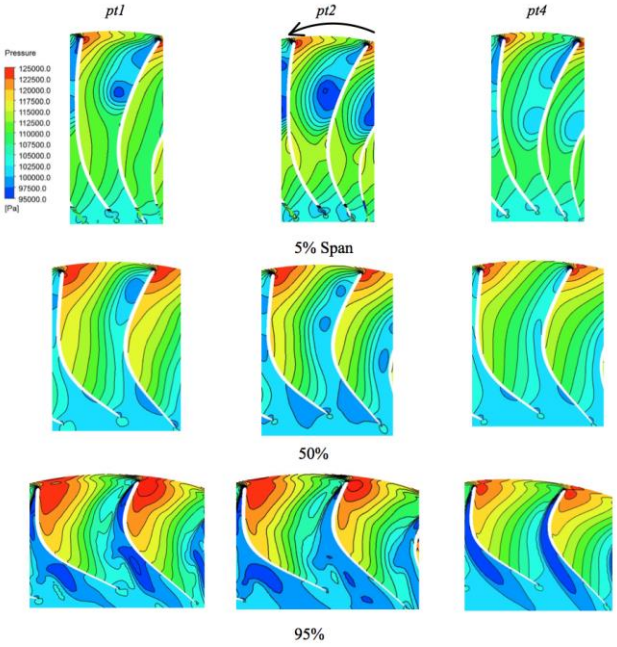

Figure 7 Pressure contour on blade-to-blade plane for pt1, pt2 and pt4

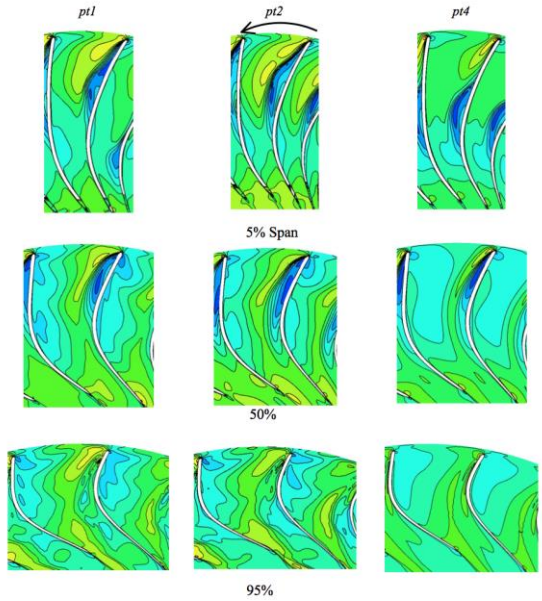

Figure 8 Velocity contour on blade-to-blade plane for pt1, pt2 and pt4

This behaviour is still visible at 50% spanwise location. However this particular feature at mid-span is not unique to pulsating condition since it also exists during steady operations. Meanwhile, close to the shroud wall, the low velocity region ceases to exist close to the suction surface leading edge but has mitigated downstream for pt3. For pt1 and pt2, the low velocity now occurred close to the leading edge pressure surface.

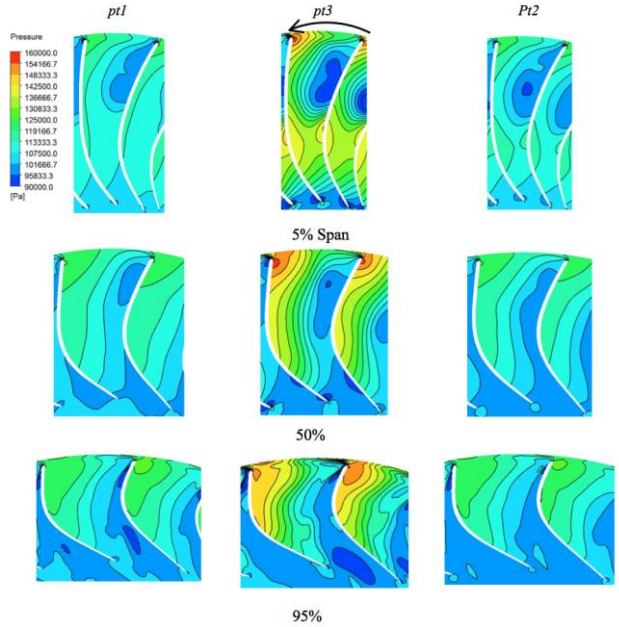

Figure 9 Pressure contour on blade-to-blade plane for pt1, pt3 and pt2

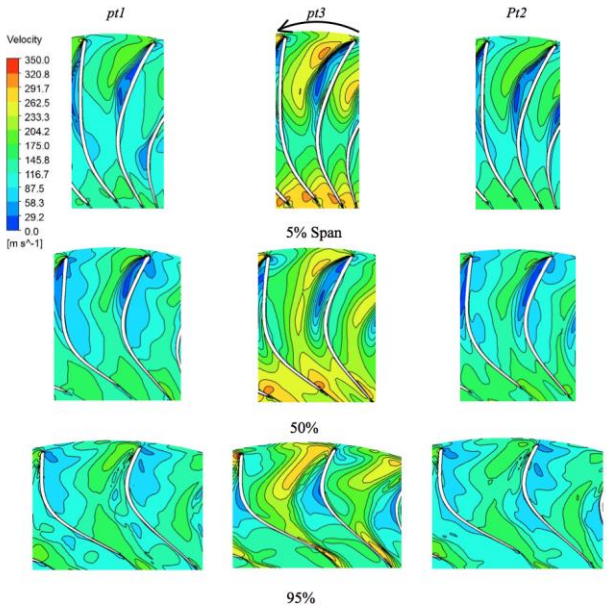

Figure 10 Velocity contour on blade-to-blade plane for pt1, pt3 and pt2

4.0 CONCLUSION

The numerical model for a full stage turbocharger turbine has been successfully modelled and validated. Maximum RMS recorded for comparison of CFD and experimental data for both mass flow parameter and efficiency is 2%. Results indicated that at similar total pressure at the turbine inlet, there are

significant that exist in the pressure distribution between increment and decrement pressure period as well as during steady state conditions. It has also been found that the flow field behaviour is more unorganized during pulsating flow operation as compared to its steady state counterpart. The flow separation close the suction surface near the shroud have been found to occur much earlier during pulsating condition as compared to the steady state operation. Moreover, during the pressure decrement period, results indicated that the secondary flow that exist close to the shroud has created large flow blockage that extend up to 50% of the passage width. This in turns result in the reduction of the turbine capability to generate torque at the particular location.

Acknowledgement

The corresponding author would like to acknowledge Universiti Teknologi Malaysia (VOT number: Q.J130000.2724.01K70) for the financial support on this research.

Nomenclature

$\dot{m}$	mass flow rate (kg/s)
T	temperature (K)
P	pressure (Pa)
N	rotational Speed (rpm)
ρ	density (kg/m^3)
t	time (s)
U	velocity (m/s)
τ	torque (Nm)
C	isentropic velocity (m/s)

Subscript

01	inlet
5	exit
act	Actual
Isen, is	Isentropic

References

[1] J. W. Lam, Q. D. H. Roberts, and G. T. McDonnel. 2002. Flow Modelling of a Turbocharger Turbine Under Pulsating Flow, *Preceedings IMechE Int. Conf. Turbochargers Turbocharging (Mechanical Eng. Publ. London)*. 181–197.

[2] D. Palfreyman and R. F. Martinez-Botas. 2004. The Pulsating Flow Field in a Mixed Flow Turbocharger Turbine: An Experimental and Computational Study. *Proceedings of the ASME Turbo Expo 2004*. 5:697–708.

[3] N. Karamanis, R. F. Martinez-Botas, and C. C. Su. 2001. Mixed Flow Turbines: Inlet and Exit Flow Under Steady and Pulsating Conditions. *J. Turbomach.* 123(2):359.

[4] F. Hellstrom and L. Fuchs. 2008. Effects of Inlet Conditions on the Turbine Performance of a Radial Turbine. *Turbomachinery, Parts A, B, and C*. 6:1985–2001.

[5] M. H. Padzillah, S. Rajoo, M. Yang, and R. F. Martinez-Botas. 2015. Influence of Pulsating Flow Frequencies Towards the Flow Angle Distributions of an Automotive Turbocharger Mixed-flow Turbine. *Energy Conversion and Management*. 98:449–462.

[6] M. H. Padzillah, S. Rajoo, and R. F. Martinez-Botas. 2015. Flow Field Analysis of an Automotive Mixed Flow Turbocharger Turbine, *Jurnal Teknologi.* 77(8): 21–27.

[7] M. H. Padzillah, S. Rajoo, and R. F. Martinez-Botas. 2012. Numerical Assessment of Unsteady Flow Effects on a Nozzled Turbocharger Turbine. *Proc ASME Turbo Expo Paper No. GT2012-69062.* 8:745-756.

[8] C. D. Copeland, R. Martinez-Botas, and M. Seiler. 2011. Comparison Between Steady and Unsteady Double-Entry Turbine Performance Using the Quasi-Steady Assumption. *Journal of Turbomachinery*. 133(3):031001.

[9] C. D. Copeland, R. Martinez-Botas, and M. Seiler. 2008. Unsteady Performance of a Double Entry Turbocharger Turbine With a Comparison to Steady Flow Conditions. *Volume 6: Turbomachinery, Parts A, B, and C*. 6:1579–1588

[10] C. D. Copeland, P. J. Newton, R. Martinez-Botas and M. Seiler. 2010. The Effect of Unequal Admission on the Performance and Loss Generation in a Double-Entry Turbocharger Turbine. *Proc ASME Turbo Expo No. GT2010-22212*.

[11] P. Newton, R. Martinez-Botas, and M. Seiler. 2014. A Three-Dimensional Computational Study of Pulsating Flow Inside a Double Entry Turbine. *Journal of Turbomachinery.* 137(3):031001.

[12] A. Dale and N. Watson. 1986. Vaneless Radial Turbocharger Turbine Performance. *Proc. IMechE Int. Conf. Turbocharging Turbochargers.* 65–76.

[13] S. Szymko. 2006. The Development Of An Eddy Current Dynamometer For Evaluation Of Steady And Pulsating Turbocharger Turbine Performance, Imperial College of Science, Technology and Medicine, University of London.

[14] S. Rajoo and R. Martinez-Botas. 2006. Experimental Study On The Performance Of A Variable Geometry Mixed Flow Turbine For Automotive turbocharger. *8th International Conference on Turbochargers and Turbocharging*. 183–192.

[15] M. Abidat. 1991. Design and Testing of a Highly Loaded Mixed Flow Turbine, Imperial College of Science, Technology and Medicine, University of London.